Hindawi
Adsorption Science & Technology
Volume 2023, Article ID 6473526, 9 pages
https://doi.org/10.1155/2023/6473526

Research Article

Recovery of Palladium from Acidic Solution Using Polyethylenimine-Crosslinked Calcium Silicate Hydrate Derived from Oyster Shell Waste: Adsorption and Mechanisms

Su Bin Kang[1], **Zhuo Wang**[1], **and Sung Wook Won**[1,2]

[1]*Department of Ocean System Engineering, Gyeongsang National University, 2 Tongyeonghaean-ro, Tongyeong, Gyeongnam 53064, Republic of Korea*
[2]*Department of Marine Environmental Engineering, Gyeongsang National University, 2 Tongyeonghaean-ro, Tongyeong, Gyeongnam 53064, Republic of Korea*

Correspondence should be addressed to Sung Wook Won; sungukw@gmail.com

Received 26 May 2022; Revised 6 August 2022; Accepted 13 October 2022; Published 15 April 2023

Academic Editor: Hesham Hamad

In this work, a new adsorbent with effective Pd(II) adsorption ability was synthesized using an oyster shell and fumed silica as the matrix materials and polyethyleneimine as the functional ligand. The adsorption performance of the developed adsorbent was evaluated for the recovery of palladium chloride ions (Pd(II)) from strong acid solutions. To understand the characteristics of the materials used in the study, samples were characterized by Fourier transform infrared spectroscopy (FT-IR), transmission electron microscopy (TEM), X-ray diffraction (XRD), and zeta potential analysis. Zeta potential analysis revealed that the isoelectric point of polyethylenimine-crosslinked calcium silicate hydrate (PEI-CSH) was 9.85. Isotherm experiments revealed that the maximum Pd(II) uptake estimated by the Langmuir model was 156.03 mg/g, which was 22.4 and 35.6 times higher than that of the oyster shell powder (OSP) and calcium silicate hydrate (CSH), respectively. The Pd(II) adsorption equilibrium was established in 180 minutes, according to kinetic experiments. These results suggested the possibility of Pd(II) recovery from oyster shell-based adsorbent. Through five adsorption and desorption cycles, the reusability of PEI-CSH was confirmed. PEI-CSH can therefore be considered a potential adsorbent for Pd(II) recovery.

1. Introduction

Palladium (Pd) has been widely used in automotive catalytic converters, jewellery, bimetallic catalysts, multilayer ceramic capacitors, fuel cell catalysis, and medical industries due to its unique properties [1–6]. With the rapid development of modern society, the demand for Pd is continuously increasing. But because of steady and constrained production, palladium is in greater demand than it is available [7, 8]. The ore only contains 2–6 g/t of Pd, but commonly phased out products like printed circuit boards and car catalytic converters have 100–10,000 g/t of Pd on average [9]. Therefore, the recovery of Pd from final items is therefore extremely important.

Leaching is commonly used to extract palladium from solid wastes, where large amounts of palladium-containing wastewater are generated. Recovery of Pd from wastewater is not only economically beneficial but also important in terms of public health, as excess Pd in water can have negative effects on human health. Consuming too much Pd can cause asthma, cancer, renal failure, and other illnesses [10–12]. Some methods such as ion exchange [13], hydrometallurgy [14], and solvent extraction [15] have been used to recover and reduce the Pd concentration in wastewater; nonetheless, there are several drawbacks to these techniques, including high running costs and poor efficiency. Pd is thus transmitted from improperly treated industrial effluent that contains Pd to water bodies like rivers and lakes, having a

negative impact on human and animal health. Therefore, it is vital to investigate low-cost and efficient Pd recovery techniques. Adsorption was therefore presented as a possible alternative for the recovery of palladium from wastewater since it overcomes the aforementioned drawbacks.

Natural materials often have complex hierarchical structures and thus can be used as adsorbent materials [16, 17]. A number of researchers have paid attention to the development of functional materials for environmental applications using agriculture [18], biological [19], and fermented [20] wastes. Oyster shell (OS) is an abundant biowaste that has attracted much attention [21]. It has been applied to remove heavy metals such as Ni(II) [22], Hg(II) [23], and Cd(II) [24] from wastewater. However, OS has low adsorption capacity and weak acid resistance, so there are limitations in treating acidic wastewater directly with OS. Aqua regia is commonly used to leach Pd from obsolete products, and the leachate is strongly acidic with large amounts of chloride ions. In order to use OS as an adsorbent for Pd recovery from acid solutions, the problem of low acid resistance must first be solved. Since OS (whose main component is $CaCO_3$) and fumed silica can be converted to acid-insoluble calcium silicate hydrate (CSH) by calcination, the conversion of OS to CSH can be an effective way to compensate for the disadvantages of OS when it is used as an adsorbent [25]. In previous studies, the preparation of CSH involves the utilization of expensive and toxic chemical reagents [26–28]. Here, OS, an abundant biowaste, was used to replace commercial calcium chloride and no toxic solvent was used in the preparation of CSH. Pd(II) exists mainly in the form of $PdCl_4^{2-}$ among several Pd-chloride complexes in strong acid solutions containing lots of chloride ions [29]. On the other hand, CHS synthesized from OS does not have a functional group capable of binding to $PdCl_4^{2-}$. Therefore, it is necessary to apply appropriate surface modification methods to greatly improve the adsorption capacity of CSH towards Pd(II). An amine-rich polymer known as polyethylenimine has been extensively employed to alter adsorbents for the recovery of precious metals including P(II), Pt(IV), and Au(III) [9, 30, 31].

In this study, a polyethylenimine-crosslinked CSH (PEI-CSH) adsorbent for Pd(II) recovery was successfully prepared by crosslinking polyethylenimine (PEI) on the surface of CSH synthesized from OS. Characteristic properties of PEI-CSH were identified through FT-IR, XRD, zeta potential analysis, and TEM. The basic interaction between PEI-CSH and Pd(II) was confirmed by batch experiments. Adsorption isotherm experiments and kinetic experiments were also performed to investigate the adsorption ability of Pd(II) on PEI-CSH.

2. Materials and Methods

2.1. Materials. Palladium(II) chloride (purity: 99.0%) was purchased from Kojima Chemicals Co., Ltd. (Saitama, Japan). OS waste was collected from a local market in Tongyeong, South Korea. Branched PEI (M_w: 70,000, content: 50%) was supplied by Habjung Moolsan Co., Ltd. (Seoul, Korea). 3-Aminopropyltriethoxysilane (APTES, 99%) was provided by Daejung Chemical & Metals Co., Ltd. (Siheung, Korea). Fumed silica was purchased from Sigma-Aldrich Korea Ltd. (Yongin, Korea). Glutaraldehyde (GA, 25% solution, extra pure) was supplied by Junsei Chemical Co., Ltd. (Tokyo, Japan). Other reagents such as ethanol, NaOH, and HCl used in this study were of analytical grade.

2.2. Preparation of PEI-CSH. To eliminate contaminants and silt, OS trash was first thoroughly cleaned with distilled water, followed by a day of drying in an air-drying oven. The washed OS was soaked in 5% sodium hypochlorite (NaClO) solution for 24 h to get rid of organic matters attached on the surface, then washed with distilled water, followed by a thorough drying. The dried OS was crushed by a ball mill (DW BM915, Dongwon Scientific System Co., Korea) with alumina balls at 500 rpm to produce oyster shell powder (OSP). The OSP (particle size < 90 μm) was collected through sieving. In order to manufacture CSH, a 1 : 1.2 weight ratio of OSP and fumed silica was combined. This mixture was then calcined at 800°C for 6 h. [25].

PEI-CSH was prepared based on previously reported methods with slight modification [32, 33]. Briefly, CSH (3 g) and APTES (3 mL) were added to 300 mL of 30% ethanol 300 mL and stirred at 25°C for 24 h. Then, the APTES-treated CSH was collected by filtration, washed with ethanol several times, and dried overnight at 100°C. Finally, PEI-CSH was produced by mixing 1% PEI solution with APTES-CSH at 40°C for 24 h, during which 1 mL of 25% GA was added dropwise. The produced PEI-CSH was repeatedly washed in deionized water, dried for 24 hours in an oven at 40°C, and then kept in a desiccator for further use.

2.3. Analytical Methods. The IR spectra of OSP, CSH, and PEI-CSH were investigated using a FT-IR spectrometer in the range of 4000–400 cm^{-1} (Nicolet IS50, Thermo Fisher, USA). The compositions of OSP, CSH, and PEI-CSH were analyzed using XRD (D8 Advance A25, Bruker, USA) with Cu Kα radiation ($\lambda = 1.54$ Å) and 2θ range from 10° to 70°. A zeta potential analyzer was used to examine the zeta potential of CSH and PEI-CSH at various pH levels (ELSZ-2000, Otsuka, Japan). The surface morphologies of OSP, CSH, and PEI-CSH were observed by 300 kV TEM (Tecnai TF30, FEI, USA) at ×195,000 magnification.

2.4. Batch Adsorption and Desorption Experiments. The Pd(II) stock solution (1000 mg/L) was made by dissolving a particular amount of Pd(II) in 0.01 M HCl, and the Pd(II) concentrations used in this study were made by diluting the Pd(II) stock solution. Adsorption isotherm tests were conducted in the range of starting Pd(II) concentrations from 30 to 700 mg/L in order to determine the maximum adsorption capacity of the adsorbent for Pd(II). A shaking incubator was used to stir a 50 mL conical tube containing 0.06 g of adsorbent and 30 mL of Pd(II) solution for 24 hours at room temperature (25°C) and 160 rpm. Samples from the supernatant were taken after equilibrium to determine the final Pd content (II). At predetermined intervals during the

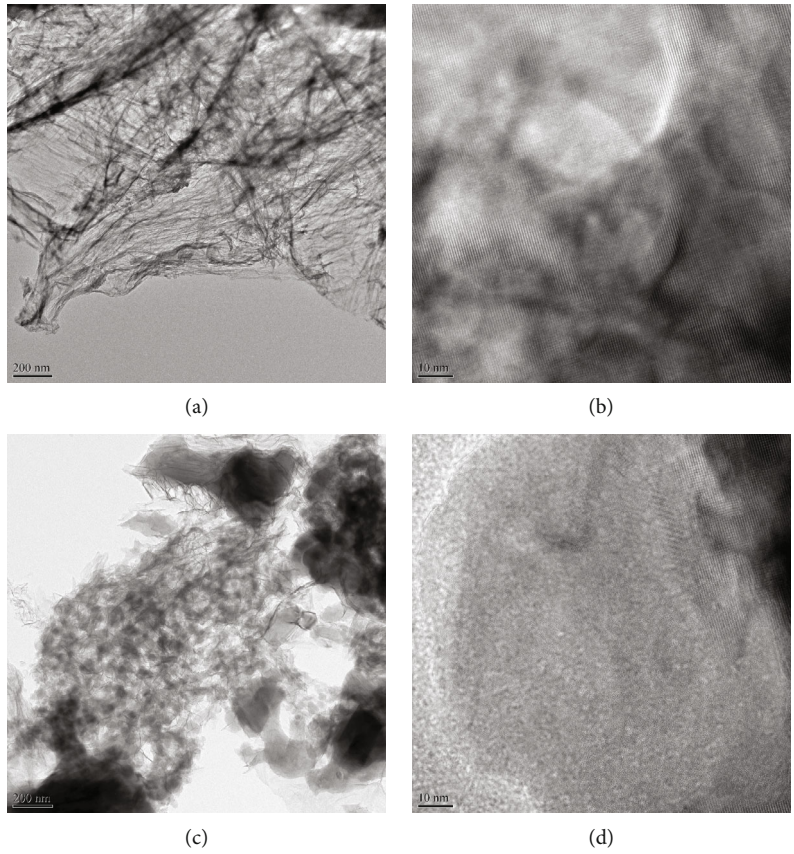

(a) (b)

(c) (d)

Figure 1: TEM images of (a, b) CSH and (c, d) PEI-CSH at 12,000x (a, c) and 195,000x (b, d) magnification.

kinetic studies, samples from the supernatant were taken for concentration measurement at an initial Pd(II) concentration of 200 mg/L. All the samples were taken in triplicate. The obtained samples were diluted accordingly with tertiary distilled water after being centrifuged for 10 min at 10,000 rpm. ICP-OES (Avio200, PerkinElmer, USA) was used to detect the residual Pd(II) concentration, and Equation (1) was used to determine the Pd(II) adsorption quantity q (mg/g).

$$q = \frac{(C_i - C_f)V}{m}, \tag{1}$$

where the initial and final Pd(II) concentrations, the working volume, and the weight of the adsorbent are expressed by C_i and C_f (mg/L), V (L), and m (g), respectively.

Prior to the desorption experiment, Pd(II)-loaded PEI-CSH was made by mixing 0.06 g of PEI-CSH with 30 mL of 200 ppm Pd(II) solution in a 50 mL conical tube. This adsorbent was promptly rinsed with deionized water and then resuspended in the eluent, which was a mixed solution of 0.01 M HCl and 0.01 M thiourea. A total of five repetitions were done for the adsorption and desorption cycles mentioned above. Following the proper dilution of the samples obtained from adsorption and desorption studies, the Pd(II) content of the samples was determined using an ICP-OES. The desorption efficiency was determined using the subsequent equation.

$$\text{Efficiency of desorption (\%)} = \frac{\text{Released Pd(II) weight (mg)}}{\text{Initially adsorbed Pd(II) weight (mg)}} \times 100. \tag{2}$$

3. Results and Discussion

3.1. Characterization

3.1.1. TEM Image. To explore the shape and crystal structure of the CSH-based adsorbent, TEM examination of CSH and PEI-CSH was performed. CSH composites with a hierarchical structure can be obtained by hydrothermal reaction of the OS and fumed silica (Figure 1(a)). Moreover, a close-up image of the CSH lattice is presented in Figure 1(b), which exhibits a small grid shape, suggesting that the precursors are formed along calcium and oxygen sheets surrounded by tetrahedral silica chains. Moreover, CSH demonstrate that channels are arranged orderly and uniformly [34]. After crosslinking with PEI, the hierarchical structure disappeared as shown in Figure 1(c). In the magnified image (Figure 1(d).), the surface of PEI-CSH is covered with polymer, and only a partial lattice pattern is observed. It indicates that during the preparation process,

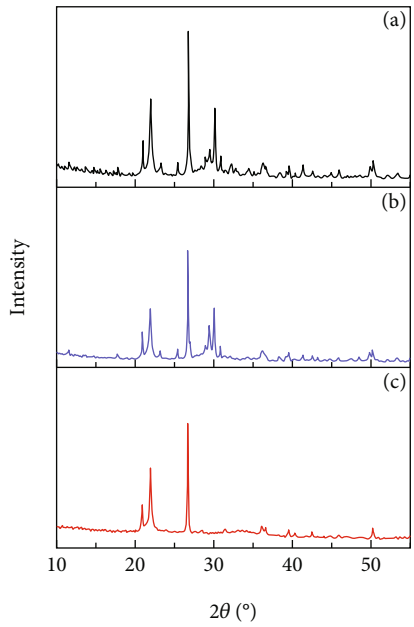

Figure 2: X-ray diffraction patterns of (a) CSH, (b) PEI-CSH, and (c) Pd-loaded PEI-CSH.

the intrinsic properties of CSH were not destroyed, as well as the PEI functional ligands were successfully bound to the CSH surface.

3.1.2. XRD Analysis. In Figure 2, the entire XRD pattern peaks are strong, indicating that the substance is highly crystallized. The characteristic peaks of CSH occur at 20°–30° and 50.8° [35, 36]. The grafting of PEI to the CSH surface may be the cause of the observed drop in the main peak diffraction intensity for PEI-CSH. After adsorption process, one of the main peaks disappeared. The missing peak was located at 29.8°, which is considered to be the effect of Pd(II)-induced destructive interference [37].

3.1.3. FT-IR Analysis. The FT-IR is a crucial tool for analyzing changes in chemical bonds in materials as well as potential interactions between metal ions and the surface functional groups of adsorbents. The FT-IR spectra of CSH, PEI-CSH, and Pd-loaded PEI-CSH are presented in Figure 3. As shown in Figure 3(a), the peaks in the range of 1200–400 cm^{-1} represent the chemical bonds in the silica chains [38]. The peaks at 961, 641, and 443 cm^{-1} were assigned to Si-O (asymmetric stretching vibration), Si-O-Si (out-of-plane bending vibration), and O-Si-O (in-plane bending vibration), respectively [39]. After PEI coating, the peaks at 961, 643, and 443 cm^{-1} were shifted to 963, 643, and 451 cm^{-1}, respectively (Figure 3(b)). There were four new peaks found at 1073, 902, 796, and 697 cm^{-1}. The peak at 1073 cm^{-1} was assigned to the C-N stretching vibration of aliphatic amines [40]. The band associated with amines was seen in the 910-665 cm^{-1} range. Only primary and secondary amines were shown to have this robust, wide band, which was caused by N-H wagging [41]. Therefore, it can be explained that PEI was successfully crosslinked to the CSH surface. After the adsorption of Pd(II) (Figure 3(c)),

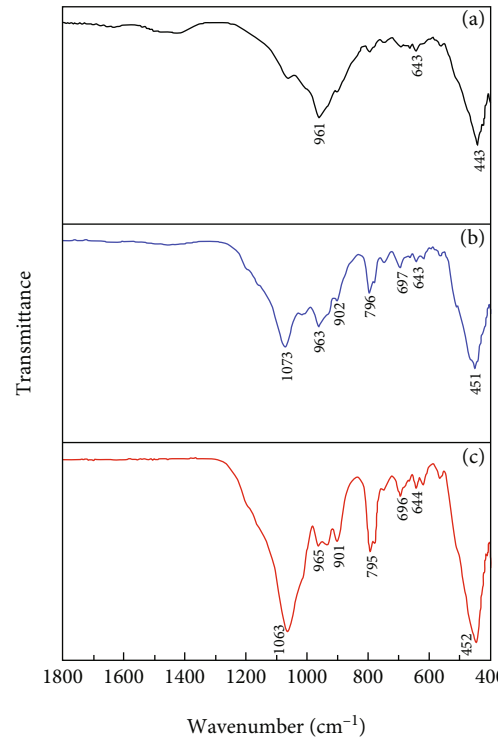

Figure 3: FT-IR spectra of (a) CSH, (b) PEI-CSH, and (c) Pd-loaded PEI-CSH.

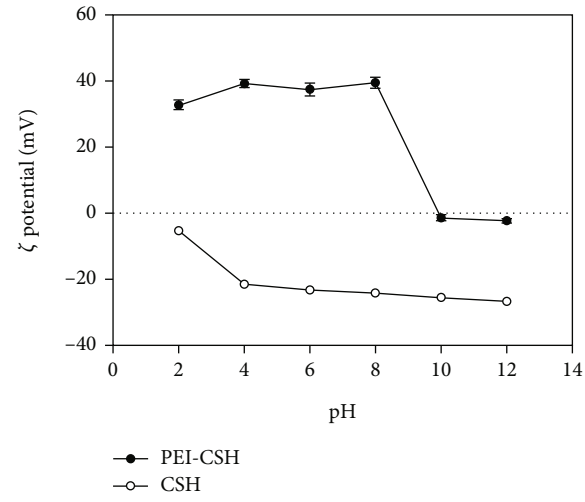

Figure 4: Surface zeta potential of CSH and PEI-CSH with different pH values.

the peaks at 1073, 902, 796, and 697 cm^{-1} shifted slightly, and the intensity also changed. This change can be considered a result of the involvement of the amine group in the adsorption process [42].

3.1.4. Zeta Potential. According to Figure 4, the zeta potential of CSH decreased from -5.32 to -26.70 mV, with the pH value increasing from 2 to 12. On the other hand, PEI-CSH showed a high positive charge of +32.77 mV at below pH 8 and negative charge at -1.40 mV at above pH 10. In

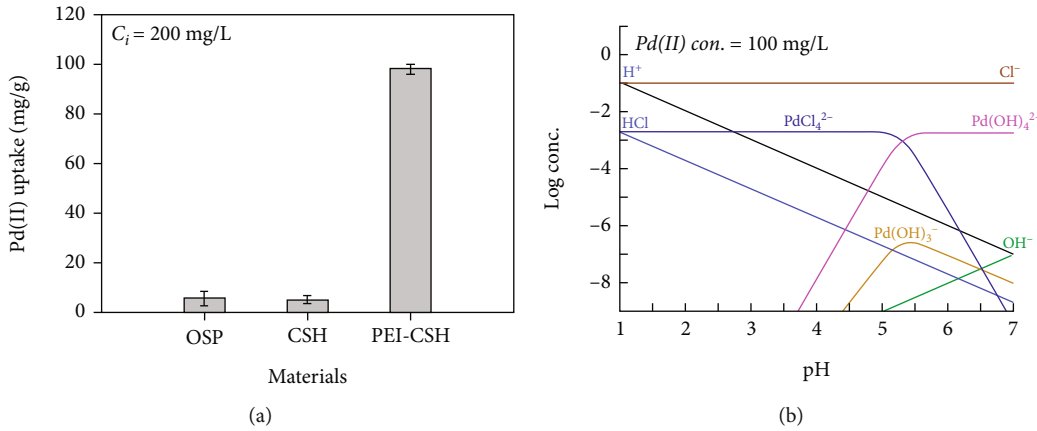

Figure 5: (a) Adsorption of Pd(II) onto different samples (OSP, CSH, and PEI-CSH) (experimental conditions: pH 2; volume of solution, 30 mL; mass of adsorbent, 60 mg; and initial Pd(II) concentration, 200 mg/L). (b) Pd(II)-pH equilibrium diagram for system hydrochloric acid (condition).

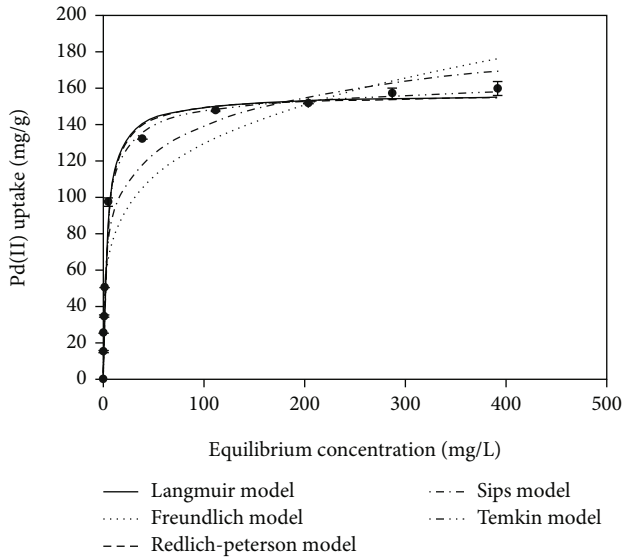

Figure 6: The isotherm models for Pd(II) adsorption onto PEI-CSH (experimental conditions: pH 2; volume of solution, 30 mL; mass of adsorbent, 60 mg; and initial Pd(II) concentration range, 30-700 mg/L).

Table 1: Isotherm parameters of Pd(II) adsorption onto PEI-CSH.

Models	Parameter	Value
Langmuir	q_{max} (mg/g)	156.03
	b_L (L/mg)	0.2344
	R^2	0.994
Freundlich	K_F (L/g)	46.34
	n	4.47
	R^2	0.913
Sips	q_{max} (mg/g)	156.68
	K_S (L/mg)	0.2374
	n	1.0288
	R^2	0.994
Redlich-Peterson	K_R (L/g)	40.2145
	α_R (L/mg)	0.3005
	β	0.9707
	R^2	0.991
Temkin	K_T (L/mg)	5.1132
	b_T (J/mol)	110.8861
	R^2	0.976

addition, the isoelectric point (PI) of PEI-CSH was 9.85, which was present at a higher pH than that of CSH. Consequently, the surface of PEI-CSH is positively charged at a pH lower than PI, which can be considered due to the amine groups such as -NH^+, -NH_2^+, and NH_3^+ in PEI coated on CSH.

3.2. Adsorption Mechanism. A large number of amine groups were produced on the surface of CSH as a result of PEI grafting onto CSH to generate PEI-CSH. The adsorption capacity of PEI-CSH for Pd(II) was significantly increased at pH 2 when amine groups were concentrated on the adsorbent surface (Figure 5(a)). The Pd(II) uptake of PEI-CSH was 99.54 mg/g, which is very high compared to that of OSP (6.97 mg/g) and CSH (4.38 mg/g). Interestingly, the difference in the amount of Pd(II) adsorption before and after the introduction of PEI into CSH is about 22.7-fold. As such, the presence/absence of PEI in the adsorbent largely affected the Pd(II) adsorption amount. To explain this result, it is necessary to check the form of Pd(II) at pH 2. As shown in Figure 5(b), Pd(II) exists as an anion in the form of $PdCl_4^{2-}$ in acidic conditions. Therefore, the anionic Pd(II) is likely to be bound with the positively charged amine groups in PEI-CSH through electrostatic attraction, which has been proved in our previous work [32].

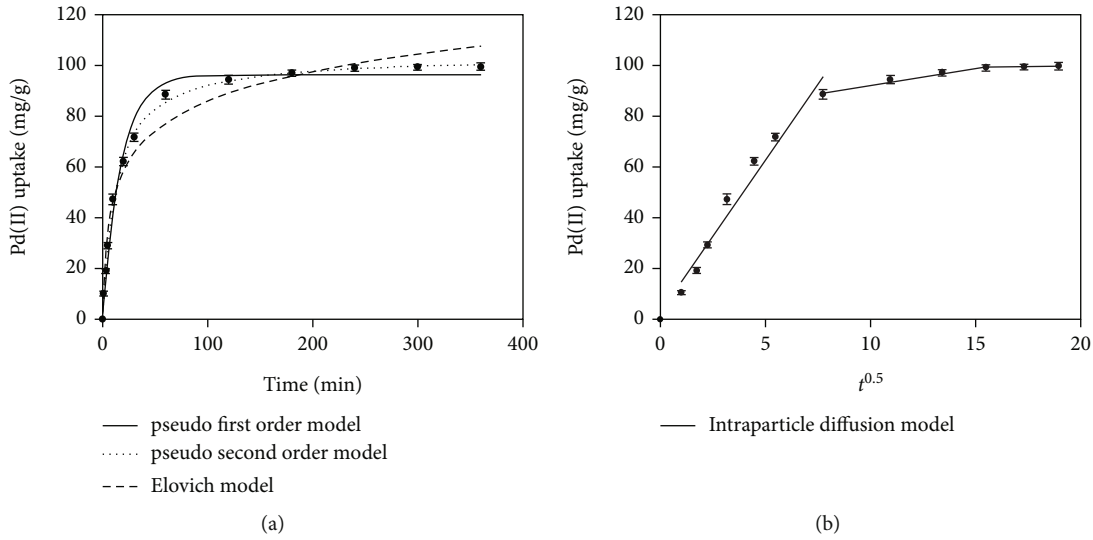

Figure 7: (a) The PFO, PSO, Elovich, and (b) intraparticle diffusion models for Pd(II) adsorption onto PEI-CSH (experimental conditions: pH 2; volume of solution, 60 mL; mass of adsorbent, 120 mg; and initial Pd(II) concentration, 200 mg/L).

3.3. Adsorption Isotherms and Modeling. To determine the maximal Pd adsorption capacity of PEI-CSH, isothermal adsorption studies were carried out at pH 2 (II). According to Figure 6, the PEI-Pd(II) CSH's uptakes increased as Pd(II) concentrations rose before reaching their maximum adsorption capacity. Adsorption isotherm models can offer crucial details on the adsorption process, surface characteristics, and interactions between the adsorbent and adsorbate. The experimental data were described by Langmuir, Freundlich, Sips, Redlich-Peterson, and Temkin isotherm models (see Supporting Information (available here)), and the corresponding parameters are listed in Table 1.

The Langmuir and Sips models had greater coefficient of determination (R^2) values than the other models, indicating that they were more suited to explain the adsorption of PEI-CSH for Pd(II) [6]. According to the Langmuir model, PEI-CSH was adsorbed on Pd(II) in a monolayer [43]. The R_L values fell between 0 and 1, indicating that PEI-CSH adsorption for Pd(II) was favorable [44]. According to the Sips model, the PEI-Pd(II) CSH's adsorption process combines monolayer adsorption at high Pd(II) concentrations with diffusion at low Pd(II) concentrations [9]. Combining the Langmuir and Freundlich equations creates the Redlich-Peterson model. A value of 40.21 was determined for the Redlich-Peterson rate constant (K_R). The result was close to 1, indicating that the Pd(II) isotherms are compatible with the Langmuir and Redlich-Peterson models and that they are near to the Langmuir form [45]. According to the Temkin model, all molecules in the layer will experience a linear drop in the heat of adsorption as the layer's coverage increases due to the adsorbate-adsorbent interaction. As a result, the adsorption exhibits a consistent binding energy distribution up to a maximum level [46]. The exothermic nature of the adsorption process was suggested by the positive Temkin constant (b_T) value [9].

3.4. Adsorption Kinetics and Modeling. One of the key elements in determining the effectiveness of the overall adsorption process is adsorption kinetics, which also offers theoretical understanding of the reaction pathways and processes of adsorption [47]. To determine the time at which Pd(II) adsorption on PEI-CSH reaches equilibrium, the impact of contact time was assessed. The studies were conducted in an acidic environment (pH = 2) for 360 min at 25°C with an initial Pd(II) concentration of 200 mg/L. In the acidic setting, as shown in Figure 7, PEI-CSH adsorbed 95% of the Pd(II) during the first 120 min, reaching equilibrium at 180 min, demonstrating a very fast adsorption rate.

The pseudo-first-order (PFO), pseudo-second-order (PSO), Elovich, and intraparticle diffusion models (see Supporting Information) were used to explain kinetic data. Figure 7 and Table 2 show the fitting curves and accompanying parameters.

The parameters of kinetic models as well as R^2 values and h are presented in Table 2. The experimental results confirmed that the PSO model, which had R^2 values near to unity, better suited the Pd(II) adsorption data when compared to the PFO and Elovich kinetic models. Additionally, the PSO model's projected value for the Pd(II) uptake at equilibrium, q_2, was quite similar to the experimental finding (99.67 mg/g). Since Pd(II) adsorption by PEI-CSH is a kinetic process, the PSO model proved effective in fitting the experimental data. It also suggests that chemisorption dominates physisorption during the adsorption process [48]. The chemisorption process is typically explained by the Elovich model [49]. The R^2 values of the Elovich model was 0.976, suggesting that chemisorption predominated in the adsorption process and that the model was acceptable for representing the kinetic adsorption process [49]. The three steps of the adsorption process are typically (1) film or external diffusion, (2) pore or intraparticle diffusion, and (3) adsorbate deposited on the adsorption site [50].

Table 2: Kinetic parameters of Pd(II) adsorption onto PEI-CSH.

Models	Parameter	Value
PFO	q_1 (mg/g)	96.43
	k_1 (L/min)	0.0564
	R^2	0.966
PSO	q_2 (mg/g)	100.10
	k_2	0.0008
	h	8.65
	R^2	0.998
Elovich	α (mg/g•min)	27.1856
	β (g/mg)	0.0590
	R^2	0.976
Intraparticle diffusion		
First stage	k_{p1} (mg/g•min$^{0.5}$)	12.0042
	C_1 (mg/g)	2.5736
	R^2	0.964
Second stage	k_{p2} (mg/g•min$^{0.5}$)	1.3402
	C_2 (mg/g)	78.8017
	R^2	0.976
Third stage	k_{p3} (mg/g•min$^{0.5}$)	0.1813
	C_3 (mg/g)	96.2293
	R^2	0.999

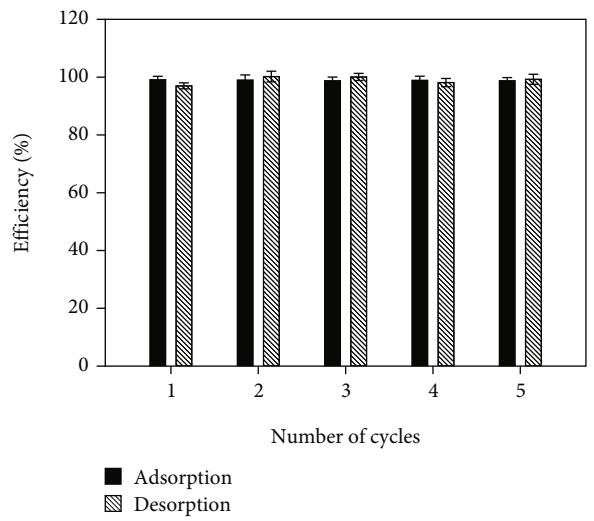

Figure 8: Repeated adsorption-desorption of Pd(II) on PEI-CSH in a batch process (adsorption conditions: pH 2; volume of solution, 30 mL; mass of adsorbent, 60 mg; initial Pd(II) concentration, 200 mg/L, desorption conditions: pH 2; volume of 0.01 M thiourea solution, 30 mL; and mass of Pd(II)-loaded adsorbent, 60 mg).

The rate-limiting phases of the adsorption process were identified using the intraparticle diffusion model. The results of q_t vs. $t^{0.5}$ acquired from the Pd(II) adsorption experiment are displayed in Figure 7(b). Three separate stages were used to display the linear plot. Since the initial step did not go through the origin, it is likely that external diffusion and subsequently intraparticle diffusion were used preferentially to regulate the adsorption of Pd(II) on PEI-CSH until equilibrium was reached [51].

3.5. Reusability of PEI-CSH. For promising adsorbents, the capacity to be reused is a crucial characteristic. Adsorbent replacement cycles can be extended, and financial gain can be made if an exhausted adsorbent can be recycled. Each of the adsorption and desorption experiments was conducted up to five times. An acidified thiourea solution prepared by mixing 0.01 M HCl and 0.01 M thiourea was used as the eluent for desorbing Pd from the loaded adsorbent. The adsorption and desorption efficiencies were nearly constant at 100% across the five cycles, as illustrated in Figure 8. Desorption by thiourea is pH-dependent [52], and thiourea forms a coordination bond with metal ions at neutral pH but induces desorption by an anion-exchange mechanism with $PdCl_4^{2-}$ at acidic pH [32]. Since an acidified thiourea solution was used in this study, the desorption is considered to be due to anion exchange. It was also confirmed that the reusability of PEI-CSH was very excellent.

4. Conclusion

In summary, an oyster waste-based adsorbent, PEI-CSH, was developed, providing an alternative way for oyster shell waste recycling. According to the TEM image, the prepared CSH showed a hierarchical structure surface, and the PEI-CSH was covered with a polymer. As evidenced by XRD analysis, PEI-CSH was observed to have characteristic peaks of CSH, which was reduced in intensity by PEI. In addition, it was found through FT-IR analysis and one-point check adsorption experiments that the absorption performance of PEI-CSH was improved by amine groups. Modification of CSH with PEI also increased the point of zero charge to 9.85. These results revealed that the adsorbent was successfully prepared. The Langmuir model was more suitable for depicting adsorption of Pd(II) on PEI-CSH, and the maximum adsorption amount was 156.03 mg/g at pH 2. Kinetic experiment showed that the adsorption equilibrium for 200 mg/L of Pd(II) at pH 2 was reached within 180 min. According to the reusability research, PEI-CSH may be recycled at least five times without losing any of its adsorption capability. Overall, the PEI-CSH, fabricated from oyster shell waste, showed the possibility of eliminating anionic Pd(II) from a HCl solution.

Data Availability

The raw data used to support the findings of this study are available from the corresponding author upon request.

Conflicts of Interest

The authors declare that they have no conflicts of interest.

Acknowledgments

This research was supported by Basic Science Research Program through the National Research Foundation of Korea (NRF) funded by the Ministry of Education (NRF-2020R1A6A3A13068967 and NRF-2020R1F1A1065937).

Supplementary Materials

The following are the supplementary data to this article. *(Supplementary Materials)*

References

[1] Y. Liu, L. Zhang, Q. Song, and Z. Xu, "Recovery of palladium as nanoparticles from waste multilayer ceramic capacitors by potential-controlled electrodeposition," *Journal of Cleaner Production*, vol. 257, article 120370, 2020.

[2] D. A. Jadhav, P. A. Deshpande, and M. M. Ghangrekar, "Enhancing the performance of single-chambered microbial fuel cell using manganese/palladium and zirconium/palladium composite cathode catalysts," *Bioresource Technology*, vol. 238, pp. 568–574, 2017.

[3] C. Icsel, V. T. Yilmaz, F. Ari, E. Ulukaya, and W. T. A. Harrison, "*trans* -Dichloridopalladium(II) and platinum(II) complexes with 2-(hydroxymethyl)pyridine and 2-(2-hydroxyethyl)pyridine: Synthesis, structural characterization, DNA binding and *in vitro* cytotoxicity studies," *European Journal of Medicinal Chemistry*, vol. 60, pp. 386–394, 2013.

[4] A. K. Mishra and N. K. Kaushik, "Synthesis, characterization, cytotoxicity, antibacterial and antifungal evaluation of some new platinum (IV) and palladium (II) complexes of thiodiamines," *European Journal of Medicinal Chemistry*, vol. 42, no. 10, pp. 1239–1246, 2007.

[5] K. Husain, M. Abid, and A. Azam, "Synthesis, characterization and antiamoebic activity of new indole-3-carboxaldehyde thiosemicarbazones and their Pd(II) complexes," *European Journal of Medicinal Chemistry*, vol. 42, no. 10, pp. 1300–1308, 2007.

[6] B. Veisi, B. Lorestani, S. Sobhan Ardakani, M. Cheraghi, and L. Tayebi, "Post synthetic modification of magnetite @MIL-53(Fe)-NH_2 core-shell nanocomposite for magnetic solid phase extraction of ultra-trace Pd(II) ions from real samples," *International Journal of Environmental Analytical Chemistry*, pp. 1–18, 2022.

[7] A. K. Mosai, R. H. Johnson, and H. Tutu, "Modelling of palladium(II) adsorption onto amine-functionalised zeolite using a generalised surface complexation approach," *Journal of Environmental Management*, vol. 277, article 111416, 2021.

[8] D. Bourgeois, V. Lacanau, R. Mastretta, C. Contino-Pépin, and D. Meyer, "A simple process for the recovery of palladium from wastes of printed circuit boards," *Hydrometallurgy*, vol. 191, article 105241, 2020.

[9] Z. Wang, S. B. Kang, and S. W. Won, "Selective adsorption of palladium(II) from aqueous solution using epichlorohydrin crosslinked polyethylenimine-chitin adsorbent: batch and column studies," *Journal of Environmental Chemical Engineering*, vol. 9, no. 2, article 105058, 2021.

[10] C. R. M. Rao and G. S. Reddi, "Platinum group metals (PGM); occurrence, use and recent trends in their determination," *TrAC Trends in Analytical Chemistry*, vol. 19, no. 9, pp. 565–586, 2000.

[11] G. Khayatian and K. Sharifi, "Development of a dispersive liquid–liquid microextraction method for determination of palladium in water samples using dicyclohexano-18- crown-6 as extracting agent," *Journal of Inclusion Phenomena and Macrocyclic Chemistry*, vol. 79, no. 1-2, pp. 185–191, 2014.

[12] M. R. Awual and T. Yaita, "Rapid sensing and recovery of palladium(II) using *N,N*-bis(salicylidene)1,2-bis(2-aminophenylthio)ethane modified sensor ensemble adsorbent," *Sensors and Actuators B: Chemical*, vol. 183, pp. 332–341, 2013.

[13] B. Swain, J. Jeong, S.-k. Kim, and J.-c. Lee, "Separation of platinum and palladium from chloride solution by solvent extraction using Alamine 300," *Hydrometallurgy*, vol. 104, no. 1, pp. 1–7, 2010.

[14] G. Kolliopoulos, E. Balomenos, I. Giannopoulou, I. Yakoumis, and D. Panias, "Behavior of platinum group during their pyrometallurgical recovery from spent automotive catalysts," *OALib*, vol. 1, no. 5, pp. 1–9, 2014.

[15] S. Zhang, S. Ning, H. Liu, X. Wang, Y. Wei, and X. Yin, "Preparation of ion-exchange resin via in-situ polymerization for highly selective separation and continuous removal of palladium from electroplating wastewater," *Separation and Purification Technology*, vol. 258, p. 117670, 2021.

[16] Y. Du, F. Lian, and L. Zhu, "Biosorption of divalent Pb, Cd and Zn on aragonite and calcite mollusk shells," *Environmental Pollution*, vol. 159, no. 7, pp. 1763–1768, 2011.

[17] D. Ding, Y. Zhao, S. Yang et al., "Adsorption of cesium from aqueous solution using agricultural residue–walnut shell: equilibrium, kinetic and thermodynamic modeling studies," *Water Research*, vol. 47, no. 7, pp. 2563–2571, 2013.

[18] A. Othmani, S. Magdouli, P. Senthil Kumar, A. Kapoor, P. V. Chellam, and Ö. Gökkuş, "Agricultural waste materials for adsorptive removal of phenols, chromium (VI) and cadmium (II) from wastewater: a review," *Environmental Research*, vol. 204, article 111916, Part A, 2022.

[19] J. Park, S. W. Won, J. Mao, I. S. Kwak, and Y. S. Yun, "Recovery of Pd(II) from hydrochloric solution using polyallylamine hydrochloride-modified *Escherichia coli* biomass," *Journal of Hazardous Materials*, vol. 181, no. 1-3, pp. 794–800, 2010.

[20] A. Jędrczak and M. Suchowska-Kisielewicz, "A comparison of waste stability indices for mechanical–biological waste treatment and composting plants," *International Journal of Environmental Research and Public Health*, vol. 15, no. 11, p. 2585, 2018.

[21] D. Alidoust, M. Kawahigashi, S. Yoshizawa, H. Sumida, and M. Watanabe, "Mechanism of cadmium biosorption from aqueous solutions using calcined oyster shells," *Journal of Environmental Management*, vol. 150, pp. 103–110, 2015.

[22] H. Y. Yen and J. Y. Li, "Process optimization for Ni(II) removal from wastewater by calcined oyster shell powders using Taguchi method," *Journal of Environmental Management*, vol. 161, pp. 344–349, 2015.

[23] C. He, J. Qu, Z. Yu et al., "Preparation of micro-nano material composed of oyster shell/Fe_3O_4 nanoparticles/humic acid and its application in selective removal of hg(II)," *Nanomaterials*, vol. 9, no. 7, p. 953, 2019.

[24] S. Wu, L. Liang, Q. Zhang et al., "The ion-imprinted oyster shell material for targeted removal of Cd(II) from aqueous solution," *Journal of Environmental Management*, vol. 302, article 114031, Part A, 2022.

[25] J. Chen, Y. Cai, M. Clark, and Y. Yu, "Equilibrium and kinetic studies of phosphate removal from solution onto a

hydrothermally modified oyster shell material," *PLoS One*, vol. 8, no. 4, article e60243, 2013.

[26] Z. Zhang, X. Wang, H. Wang, and J. Zhao, "Removal of Pb(II) from aqueous solution using hydroxyapatite/calcium silicate hydrate (HAP/C-S-H) composite adsorbent prepared by a phosphate recovery process," *Chemical Engineering Journal*, vol. 344, pp. 53–61, 2018.

[27] N. Shao, S. Li, F. Yan, Y. Su, F. Liu, and Z. Zhang, "An all-in-one strategy for the adsorption of heavy metal ions and photodegradation of organic pollutants using steel slag-derived calcium silicate hydrate," *Journal of Hazardous Materials*, vol. 382, article 121120, 2020.

[28] Z. Zhu, Z. Wang, L. Xu et al., "Synthesis and characterization of an intermediate for C-S-H structure tailoring," *Cement and Concrete Research*, vol. 160, article 106923, 2022.

[29] C.-W. Cho, S. B. Kang, S. Kim, Y.-S. Yun, and S. W. Won, "Reusable polyethylenimine-coated polysulfone/bacterial biomass composite fiber biosorbent for recovery of Pd(II) from acidic solutions," *Chemical Engineering Journal*, vol. 302, pp. 545–551, 2016.

[30] X. Lin, D. T. Tran, M.-H. Song, and Y.-S. Yun, "Development of polyethyleneimine-starch fibers stable over the broad pH range for selective adsorption of gold from actual leachate solutions of waste electrical and electronic equipment," *Journal of Cleaner Production*, vol. 328, article 129545, 2021.

[31] H. N. Park, H. A. Choi, and S. W. Won, "Fibrous polyethylenimine/polyvinyl chloride crosslinked adsorbent for the recovery of Pt(IV) from acidic solution: adsorption, desorption and reuse performances," *Journal of Cleaner Production*, vol. 176, pp. 360–369, 2018.

[32] S. B. Kang, Z. Wang, and S. W. Won, "Application of polyethylenimine multi-coated adsorbent for Pd(II) recovery from acidic aqueous solution: batch and fixed-bed column studies," *Korean Journal of Chemical Engineering*, vol. 38, no. 3, pp. 523–530, 2021.

[33] W. You, M. Hong, H. Zhang, Q. Wu, Z. Zhuang, and Y. Yu, "Functionalized calcium silicate nanofibers with hierarchical structure derived from oyster shells and their application in heavy metal ions removal," *Physical Chemistry Chemical Physics*, vol. 18, no. 23, pp. 15564–15573, 2016.

[34] M. Schönlein and J. Plank, "A TEM study on the very early crystallization of C-S-H in the presence of polycarboxylate superplasticizers: transformation from initial C-S-H globules to nanofoils," *Cement and Concrete Research*, vol. 106, pp. 33–39, 2018.

[35] Z. Zhu, Z. Wang, Y. Zhou, Y. Wei, and A. She, "Synthesis and structure of calcium silicate hydrate (C-S-H) modified by hydroxyl-terminated polydimethylsiloxane (PDMS)," *Construction and Building Materials*, vol. 267, article 120731, 2021.

[36] U. Zulfiqar, T. Subhani, and S. W. Husain, "Synthesis and characterization of silica nanoparticles from clay," *Journal of Asian Ceramic Societies*, vol. 4, no. 1, pp. 91–96, 2016.

[37] M. M. Tarekegn, R. M. Balakrishnan, A. M. Hiruy, and A. H. Dekebo, "Removal of methylene blue dye using nano zerovalent iron, nanoclay and iron impregnated nanoclay – a comparative study," *RSC Advances*, vol. 11, no. 48, pp. 30109–30131, 2021.

[38] L. Peng, H. Dai, Y. Wu, Z. Dai, X. Li, and X. Lu, "Performance and adsorption mechanism of a magnetic calcium silicate hydrate composite for phosphate removal and recovery," *Water Science and Technology*, vol. 2017, no. 2, pp. 578–591, 2018.

[39] Y. Li, H. Li, C. Jin et al., "Multi-scale investigation and mechanism analysis on Young's modulus of C-S-H modified by multi-walled carbon nanotubes," *Construction and Building Materials*, vol. 308, p. 125079, 2021.

[40] S. Murugesh and P. Vino, "Phytochemical constituents, antioxidant activity and FT-IR analysis of *Pisonia grandis* leaf extracts," *International Journal of Pharmacognosy and Phytochemical Research*, vol. 9, no. 7, 2018.

[41] H. Xu, L. Tan, H. Cui et al., "Characterization of Pd(II) biosorption in aqueous solution by *Shewanella oneidensis* MR-1," *Journal of Molecular Liquids*, vol. 255, pp. 333–340, 2018.

[42] B. N. Bhadra, P. W. Seo, and S. H. Jhung, "Adsorption of diclofenac sodium from water using oxidized activated carbon," *Chemical Engineering Journal*, vol. 301, pp. 27–34, 2016.

[43] Y. Liu, Y. Xiong, P. Xu, Y. Pang, and C. Du, "Enhancement of Pb (II) adsorption by boron doped ordered mesoporous carbon: isotherm and kinetics modeling," *Science of the Total Environment*, vol. 708, article 134918, 2020.

[44] S. N. Jain, S. R. Tamboli, D. S. Sutar et al., "Batch and continuous studies for adsorption of anionic dye onto waste tea residue: kinetic, equilibrium, breakthrough and reusability studies," *Journal of Cleaner Production*, vol. 252, article 119778, 2020.

[45] G. M. Kim, Z. Wang, S. B. Kang, and S. W. Won, "Polyethylenimine-crosslinked chitin flake as a biosorbent for removal of Acid Blue 25," *Korean Journal of Chemical Engineering*, vol. 36, no. 9, pp. 1455–1465, 2019.

[46] A. Maleki, U. Hamesadeghi, H. Daraei et al., "Amine functionalized multi-walled carbon nanotubes: single and binary systems for high capacity dye removal," *Chemical Engineering Journal*, vol. 313, pp. 826–835, 2017.

[47] N. Ayawei, A. N. Ebelegi, and D. Wankasi, "Modelling and interpretation of adsorption isotherms," *Journal of Chemistry*, vol. 2017, Article ID 3039817, 11 pages, 2017.

[48] L. Fan, Y. Lu, L. Y. Yang, F. Huang, and X. K. Ouyang, "Fabrication of polyethylenimine-functionalized sodium alginate/cellulose nanocrystal/polyvinyl alcohol core-shell microspheres ((PVA/SA/CNC)@PEI) for diclofenac sodium adsorption," *Journal of Colloid and Interface Science*, vol. 554, pp. 48–58, 2019.

[49] L. Sun, D. Chen, S. Wan, and Z. Yu, "Performance, kinetics, and equilibrium of methylene blue adsorption on biochar derived from eucalyptus saw dust modified with citric, tartaric, and acetic acids," *Bioresource Technology*, vol. 198, pp. 300–308, 2015.

[50] U. A. Qureshi, Z. Khatri, F. Ahmed, M. Khatri, and I.-S. Kim, "Electrospun zein nanofiber as a green and recyclable adsorbent for the removal of reactive black 5 from the aqueous phase," *ACS Sustainable Chemistry & Engineering*, vol. 5, no. 5, pp. 4340–4351, 2017.

[51] R. A. Fideles, G. M. D. Ferreira, F. S. Teodoro et al., "Trimellitated sugarcane bagasse: a versatile adsorbent for removal of cationic dyes from aqueous solution. Part I: batch adsorption in a monocomponent system," *Journal of Colloid and Interface Science*, vol. 515, pp. 172–188, 2018.

[52] S. Örgül and Ü. Atalay, "Reaction chemistry of gold leaching in thiourea solution for a Turkish gold ore," *Hydrometallurgy*, vol. 67, no. 1-3, pp. 71–77, 2002.